Published in final edited form as:
J Med Chem. 2011 April 28; 54(8): 2891–2901. doi:10.1021/jm101642g.

Novel interactions of fluorinated nucleotide derivatives targeting orotidine-5′-monophosphate decarboxylase

Melissa Lewis[1], **Maria Elena Meza Avina**[1,7], **Lianhu Wei**[1], **Ian E. Crandall**[5], **Angelica Mara Bello**[1], **Ewa Poduch**[1], **Yan Liu**[4], **Christopher J. Paige**[2,3], **Kevin C. Kain**[6], **Emil F. Pai**[1,2,4], and **Lakshmi P. Kotra**[1,5,6,7,*]

[1] Center for Molecular Design and Preformulations, and Division of Cellular and Molecular Biology, Toronto General Research Institute, University Health Network, Toronto, ON, M5G 1L7 Canada

[2] Department of Medical Biophysics, Ontario Cancer Institute, Princess Margaret Hospital, 620 University Avenue, Toronto, ON, M5G 2M9, Canada

[3] Department of Immunology, University of Toronto, Toronto, Ontario, Canada

[4] Departments of Biochemistry and Molecular Genetics, University of Toronto, 1 King's College Circle, Toronto, ON, Canada

[5] Departments of Pharmaceutical Sciences and Chemistry, University of Toronto

[6] McLaughlin Center for Molecular Medicine, University of Toronto

[7] Department of Chemistry and Biochemistry, The University of North Carolina at Greensboro, Greensboro, NC 27412, USA

Abstract

Fluorinated nucleosides and nucleotides are of considerable interest to medicinal chemists due to their antiviral, anticancer, and other biological activities. However, their direct interactions at target binding sites are not well understood. A new class of 2′-deoxy-2′-fluoro-C6-substituted uridine and UMP derivatives were synthesized and evaluated as inhibitors of orotidine-5′-monophosphate decarboxylase (ODCase). These compounds were synthesized from the key intermediate, fully-protected 2′-deoxy-2′-fluorouridine. Among the synthesized compounds, 2′-deoxy-2′-fluoro-6-iodo-UMP covalently inhibited human ODCase with a second-order rate constant of $0.62 \pm 0.02\ M^{-1}sec^{-1}$. Interestingly, the 6-cyano-2′-fluoro derivative covalently interacted with ODCase defying the conventional thinking, where its ribosyl derivative undergoes transformation into BMP by ODCase. This confirms that the 2′-fluoro moiety influences the chemistry at the C6 position of the nucleotides, thus interactions in the active site of ODCase. Molecular interactions of the 2′-fluorinated nucleotides are compared to those with the 3′-fluorinated nucleotides bound to the corresponding target enzyme, and the carbohydrate moieties were shown to bind in different conformations.

Introduction

Orotidine-5′-monophosphate decarboxylase (ODCase, 4.1.1.23) catalyzes the transformation of orotidine-5′-*O*-monophosphate (OMP, **1**) to uridine-5′-*O*-monophosphate (UMP, **2**)

*Corresponding Author, Mailing address: #5-356, Toronto Medical Discoveries Tower/MaRS Center, 101 College Street, Toronto, Ontario, Canada M5G 1L7. Tel. (416) 581-7601, lkotra@uhnres.utoronto.ca.

Supplementary Information. Purity data for compounds **27–38**.

during the *de novo* synthesis of pyrimidine nucleotides (Figure 1).[1,2] UMP is a precursor for the synthesis of other pyrimidine nucleoside triphosphates, which in turn are precursors for the synthesis of ribo and deoxyribo nucleic acids. In humans, ODCase is part of the bifunctional enzyme UMP synthase, and, in lower level organisms, it is a monofunctional enzyme.[3,4,5]

In most species, including humans, pyrimidine nucleotides are obtained via *de novo* and salvage pathways. However, certain parasitic organisms, such as *Plasmodia*, are dependent on *de novo* synthesis of pyrimidine nucleotides because they do not have the necessary cellular machinery for the salvage of pyrimidine nucleotides.[6] Therefore, *de novo* pyrimidine biosynthesis is a potential target for developing novel therapeutics. *De novo* synthesis of pyrimidine nucleotides is upregulated when the demand for pyrimidine nucleotides is high, for example, during the replication of cells and during abnormal cell growth.[7,8] Thus, ODCase inhibitors could potentially exhibit a variety of biological activities including antiviral, antiplasmodial, and anticancer activities.[9] Several 5′-monophosphate analogs of classic nucleoside derivatives, such as 6-hydroxyuridine (**3**), 6-thiocarboxamidouridine (**4**), 6-azauridine (**5**), pyrazofurin (**6**), and xanthosine (**7**), are potent inhibitors of ODCase (Figure 2).[10,11,12] Interestingly, two non-nucleoside inhibitors, nifedipine and nimodipine, inhibit ODCase competitively with modest potency (Figure 2).[13,14]

Since the discovery of novel C6-substituted UMP derivatives as potent antimalarial agents, there has been interest in exploring modified nucleosides as potential ODCase inhibitors.[15,16,17,18,19,20] We reported that the monophosphate analog of 6-iodouridine (**10**) is a potent irreversible inhibitor of ODCase.[21] We showed that the mononucleotide of 6-cyanouridine (**11**) was transformed into BMP by ODCase, and the latter is a tight-binding inhibitor of ODCase. This is a novel biotransformation that does not occur chemically and was catalyzed by ODCase exclusively.[15,22,23]

Introduction of fluorine atoms onto the carbohydrate ring gives rise to interesting antiviral and anticancer activities. A number of fluorinated nucleosides are currently used in clinics including gemcitabine (**15**), L-FMAU (**16**), and F-ara-C (**17**) (Figure 2).[24,25,26,27] Gemcitabine and F-ara-C are successful anticancer agents, while L-FMAU is a potent anti-HBV drug.[28,29,30] A fluoro substitution at the C5 position of the pyrimidine moiety led to novel anticancer agents; the mononucleotide derivative of 6-azido-5-fluorouridine (**12**) inhibited human ODCase irreversibly, and its 6-amino analog (**13**) competitively inhibited ODCase at submicromolar concentrations.[17] Further investigation into 5-fluoro-6-substituted pyrimidine derivatives confirmed that 5-fluoro-6-azido-uridine and its 6-amino analog are potent compounds against various leukemia, multiple myeloma, and breast cancer cell lines.[17] The effect of the fluoro substitution on the ribosyl moiety of UMP, its conformation, and the binding interactions with ODCase have not been investigated. In this report, we reveal the synthesis, enzyme inhibition studies, and effects of 2′-fluoro-C6-substituted uridine and UMP derivatives and provide insight into fluorinated nucleoside complexes and their binding interactions.

Experimental Section

Synthesis

General—All anhydrous reactions were performed under a nitrogen atmosphere. All solvents and reagents were obtained from commercial sources; anhydrous solvents were prepared following standard procedures. Reaction progress was monitored by thin-layer chromotography (TLC; Silica gel-60 F_{254}) plates. Chromatographic purifications were performed using silica gel (60 Å, 70–230 mesh). Nuclear magnetic resonance (NMR)

spectra were recorded on a Varian spectrometer (300 and 400 MHz for ^{1}H, 75 and 100 MHz for ^{13}C, 282 or 376 MHz for ^{19}F, and 121 MHz for ^{31}P). Chemical shifts were eported in δ ppm using tetramethylsilane (TMS) as a reference for the ^{1}H NMR spectra and phosphoric acid as an external reference for ^{31}P spectra. Purities for compounds **29–32** were evaluated on a Waters Delta 660 high-performance liquid chromotography (HPLC) system attached to a photodiode array (PDA) detector equipped with a Waters Symmetry® C18 column (4.6 × 100 mm length, 5 μM). Purities for compounds **27, 28**, **33, 34**, and **38** were evaluated on a Waters™ liquid chromotography/mass spectrometry LC/MS) system equipped with a PDA detector using an XBridge C18 column (4.6 mm × 150 mm, 5 μm). Two HPLC methods were used for the purity assessment of **29–32**: method A used 15% methanol (MeOH) in H_2O (1 mL/min, isocratic), and method B used 5% MeOH in H_2O (0.5 mL/min, isocratic). Two of the following four methods were used for other compounds: method C used 10% MeOH in H_2O (1 mL/min, isocratic, for **27**, **28**, and **33**); method D used 20% MeOH in H_2O (1 mL/min, isocratic, for **28** and **38**); method E used 3% acetic acid (AcOH) in H_2O (1 mL/min, isocratic, for **34** and **38**); method F used 20% acetonitrile (CH_3CN) (with 0.05% trifluoroacetic acid (TFA)) in H_2O (1 mL/min, isocratic, for **29, 33,** and **34**). All HPLC solvents were filtered through Waters™ membrane filters (47 mm GHP 0.45 μm, Pall Corporation) and degassed with helium. Injection samples were filtered using Waters Acrodisc® syringe filters (4 mm, polytetrafluoroethylene (PTFE, 0.2 μm). All nucleotides that were tested against ODCase enzyme activity, have shown purity >95% except compound **33** exhibited upto 93% purity. Purity for compounds **35**–**37** was evaluated by elemental analysis (C, H, N) at the ANALEST Laboratory, University of Toronto, and the results were within 0.4% of the calculated values. All nucleosides evaluated in cell-based assays were >95% pure.

1-(2-Hydroxy-3, 5-di-*O*-tetrahydropyranyl-β-D-arabinofuranosyl)uracil (18): This compound was synthesized as reported earlier.[31]

2′-Deoxy-2′-fluoro-3′,5′-di-*O*-tetrahydropyranyl-β-D-uridine (19): Pyridine (24 mL) was added to a stirred solution of **18** (10 g, 24.3 mmol) in anhyd dichloromethane (120 mL) under a nitrogen atmosphere. The reaction mixture was cooled to 0°C and dimethyl aminosulfur trifluoride (DAST; 3.2 mL, 24.3 mmol) was added drop wise. After 30 min, an additional 5 equiv of DAST were added drop wise at 0°C. The reaction mixture was then stirred at 40°C overnight. The reaction mixture was cooled to 0°C, quenched with a saturated $NaHCO_3$ solution, and then extracted with dichloromethane. The combined organic layers were washed with brine, dried (Na_2SO_4), and concentrated. The crude product was purified on a Biotage SP1™ chromatography unit using a normal-phase column (EtOAc: Hexanes, 3:7–4:6) to obtain compound **19** as a yellow solid (6 g, 60% yield). ^{1}H NMR ($CDCl_3$) δ 1.45–1.94 (broad m, 12H, THP-C$\underline{H}_2$), 3.48–4.87 (broad m, 10H, THP-C$\underline{H}$-O, H-5″, H-3′, H-4′, H-5′), 4.90–5.19 (m, 1H, H-2′, $^{2}J_F$ = 52 Hz), 5.60–5.72 (4d overlap, 1H, H-5), 5.95–6.17 (4dd, 1H, H-1′, $^{3}J_F$ = 28 Hz), 7.94–8.10 (4d), 8.23 (broad s).

2′-Deoxy-2′-fluoro-6-iodo-3′,5′-di-*O*-tetrahydropyranyl-β-D-uridine (20): Compound 19 (800 g, 1.9 mmol) was dissolved in anhyd tetrahydrofuran (THF; 40 mL), and cooled to −78°C. Lithium diisopropylamide (LDA; 0.7 g, 6.7 mmol, 3.4 mL of a 2M solution in THF) was added drop wise, and the reaction mixture was stirred at −78°C for 2 h. Then, iodine (960 mg, 3.8 mmol) dissolved in anhydrous THF (15 mL) was added to the reaction mixture and stirred. After 6 h, the reaction mixture was quenched with water (25 mL), concentrated, and re-dissolved in EtOAc (50 mL). The organic phase was washed with brine, dried (Na_2SO_4), concentrated, and purified by column chromatography (hexanes:EtOAc, 1:1) to give **20** as a yellow solid (450 mg, 45% yield). ^{1}H NMR ($CDCl_3$) δ 1.29 (m, 12H), 3.40–4.80 (m, 10H), 5.47 (m, 1H, H-2′, J_{H-F}=55 Hz), 6.05 (4dd, 1H, H-1′, J_{H-F} =27 Hz), 6.45 (s, 1H, H-5).

2′-Deoxy-2′-fluoro-3′,5′-di-*O*-tetrahydropyranyl-β-D-orotidine ethyl ester (21): Compound **19** (500 mg, 1.2 mmol) in anhydrous THF (10 mL) was treated with LDA (2.5 mL, 4.6 mmol) at −78°C under a nitrogen atmosphere. Then, ethyl chloroformate (0.5 mL, 5 mmol) was added, and the reaction mixture was stirred for 2 days. The reaction was quenched with water, concentrated, and the crude product was purified on a Biotage SP1™ chromatography system using 0–50% EtOAc:hexanes as an eluent to obtain compound **21** as a yellow powder (175 mg, 30% yield). ^{1}H NMR ($CDCl_3$) δ 1.39 (t, 3H), 1.46–1.90 (broad m, 12H), 3.45–4.83 (broad m, 12H), 5.33–5.61 (m, 1H, H-2′, $J_{H–F}$=54.7 Hz), 5.81–6.02 (m, 1H, H-1′, $J_{H–F}$ = 24.9 Hz), 6.13 (4s,1H); HRMS (ESI) for $C_{22}H_{31}N_2O_9FNa$ (MNa^+), calculated: 509.1911; observed: 509.1905.

5-Bromo-2′-deoxy-2′-fluoro-3′,5′-di-*O*-tetrahydropyranyl-β-D-uridine (22): NaN_3 (5 g, 77 mmol) in water (20 mL) was added to a stirred solution of **19** (8.0 g, 19.4 mmol) in 1,2-dimethoxyethane (90 mL) at 22°C, followed by *N*-bromosuccinimide (NBS; 5.1 g, 29 mmol). The reaction mixture was stirred for 18 h. Then, the solvent was removed in vacuo, and the crude product was dissolved in water and extracted with EtOAc (300 mL × 4). The combined organic layers were dried (Na_2SO_4) and concentrated under vacuum to obtain the crude product **22** (10.8 g) as a yellow solid, which was used for the next reaction without further purification.

6-Cyano-2′-deoxy-2′-fluoro-3′, 5′-di-*O*-tetrahydropyranyl-β-D-uridine (23): NaCN (2.0 g, 41.5 mmol) was added at 22°C to a stirred solution of the crude compound **22** (6.8 g, 13.8 mmol) in anhydrous dimethylformamide (DMF; 80 mL), and the reaction mixture was stirred for 18 h. The reaction mixture was then neutralized with glacial AcOH and was concentrated under vacuum. The crude reaction mixture was dissolved in water and extracted with EtOAc (200 mL × 4). The combined organic layers were dried (Na_2SO_4) and concentrated in vacuo to obtain the crude product **23** (5.1 g) as a yellow solid, which was used in the next reaction without further purification. ^{1}H NMR ($CDCl_3$) δ 1.40–1.94 (broad m, 12H), 3.47–4.84 (broad m, 10H), 5.34–5.82 (m, 1H, H-2′, $J_{H–F}$ = 55 Hz), 5.84–6.06 (m, 1H, H-1′, $J_{H–F}$ = 26 Hz), 6.30 (d, 1H); HRMS (ESI) for $C_{20}H_{26}N_3O_7FNa$ (MNa^+), calculated: 462.1633; observed: 462.1646.

6-Amido-2′-deoxy-2′-fluoro-3′,5′-di-*O*-tetrahydropyranyl-β-D-uridine (24): Compound **23** (1.1 g, 2.5 mmol) was dissolved in 1N NaOH (10 mL), and the reaction mixture was stirred at 22°C for 1.5 h. The reaction mixture was brought to pH 6 using a 5% HCl solution and was concentrated. The concentrated reaction mixture was dissolved in water, extracted with EtOAc (100 mL × 4), the combined organic layers were dried (Na_2SO_4), concentrated, and the crude product was purified by silica gel column chromatography (5% MeOH:CH_2Cl_2) to yield compound **24** as a yellow powder (970 mg, 84% yield). ^{1}H NMR ($CDCl_3$) δ 1.40–1.94 (m, 12H), 3.45–4.88 (m, 10H), 5.34–5.82 (m, 1H, H-2′, $J_{H–F}$ = 55 Hz), 5.70–5.95 (m, 2H); HRMS (ESI) for $C_{20}H_{28}N_3O_8FNa$ (MNa^+), calculated: 480.1737; observed: 480.1752.

6-Azido-2′-deoxy-2′-fluoro-3′,5′-di-*O*-tetrahydropyranyl-β-D-uridine (25): Compound **20** (406 mg, 0.8 mmol) in anhydrous DMF (3.4 mL) was treated with sodium azide (60 mg, 0.9 mmol). The reaction mixture was stirred for 6 h at room temperature, concentrated, and dissolved in EtOAc (30 mL). The combined organic phases were washed with water (20 mL), brine (20 mL), dried (Na_2SO_4), concentrated, and purified in the dark by silica gel column chromatography (hexanes:EtOAc, 6:4→3:7) to obtain compound **25** as a yellow solid (292 mg, 85% yield). ^{1}H NMR ($CDCl_3$) δ 1.34 (m, 12H), 3.40–4.77 (m, 10H); 5.31–5.49 (m, 2H, H-5, H-2′, $J_{H–F}$=55 Hz), 6.04 (m, 1H), 8.56 (broad s, 1H).

5-Cyano-2′-deoxy-2′-fluoro-3′,5′-di-*O*-tetrahydropyranyl-β-D-uridine (26): Sodium cyanide (1.1 g, 22.2 mmol) was added to a stirred solution of compound **22** (3.7 g, 7.4 mmol) in anhydrous DMF (50 mL), and the reaction was carried out in a microwave for 5 min at 150°C. The reaction mixture was diluted with water, neutralized (AcOH), concentrated, and extracted with EtOAc (100 mL × 4). The combined organic layers were dried (Na_2SO_4) and concentrated to obtain the crude product **26** (1.2 g), which was used without further purification. HRMS (ESI) for $C_{20}H_{26}N_3O_7FNa$ (MNa^+), calculated: 462.1644; observed: 462.1646.

2′-Deoxy-2′-fluoro-6-iodo-β-D-uridine (27): Compound **20** (380 mg, 1.7 mmol) was dissolved in aqueous MeOH and treated with Amberlite (H^+) (150 mg). The reaction mixture was stirred in the dark overnight at room temperature, filtered, and concentrated. The crude product was purified by silica gel column chromatography (15% CH_3OH:$CHCl_3$) in the dark to obtain compound **27** as a light brown solid (200 mg, 78%). UV λ_{max} (MeOH) =267 nm (ε=10,856 $mol^{-1}cm^{-1}$); ^1H NMR (CD_3OD) δ 3.67 (dd, 1H), 3.87 (m, 2H), 4.53 (ddd,1H, H-3′, J_{H-F}=21 Hz), 5.43 (dd,1H, H-2′, J_{H-F}=57 Hz), 6.08 (dd, 1H, H-1′, J_{HF}=27 Hz), 6.43 (s, 1H). ^{19}F NMR (CD_3OD) δ −193.27 (ddd, J_{H-F} =57, 27, 21 Hz). HRMS (ESI) calculated for $C_9H_{10}N_2O_5FNaI$ (M+Na): 394.9510; observed: 394.9516.

Deprotection of 5- and 6-substituted 2′-fluoro nucleosides: Compounds **21, 23–26** were deprotected using the procedure described for **27** to yield compounds **28–32**, respectively.

6-Azido-2′-deoxy-2′-fluoro-β-D-uridine (28): Compound **25** was deprotected to obtain compound **28** as a pale yellow solid (100 mg, 54% yield). UV λ_{max} (MeOH) = 283 nm (ε=10,691 $mol^{-1}cm^{-1}$). ^1H NMR (CD_3OD) δ 3.61 (dd, 1H), 3.71 (m, 2H), 4.43 (ddd, 1H, H-3′, J_{H-F}=21 Hz), 5.24 (dd,1H, H-2′, J_{H-F}=56.1 Hz), 5.46 (s, 1H), 5.94 (dd, 1H, H-1′, J_{H-F}=27.5 Hz). ^{19}F NMR (CD_3OD) δ −193.32 (ddd, J =56.1, 20.1, 27.5 Hz). HRMS (ESI) calculated for $C_9H_{11}FN_5O_5$ (MH+): 288.0745, observed: 288.0748; calculated for $C_9H_{10}FN_5NaO_5$ (MNa+): 310.0564, observed: 310.0564.

6-Cyano-2′-deoxy-2′-fluoro-β-D-uridine (29): Compound **23** was deprotected to yield product **29** as a pale yellow solid (1.86 g, 82% yield). UV λ_{max} (MeOH)=278 nm ε=3209 mol^{-1} cm^{-1}); ^1H-NMR (CD_3OD) δ 3.69 (dd, 1H), 3.84–3.94 (m, 2H), 4.55 (ddd, 1H, H3′, J_{H-F} = 20 Hz), 5.45 (dd, 1H, H2′, J_{H-F} = 55 Hz), 5.88 (d, 1H, H1′, J_{H-F} = 25 Hz), 6.46 (s, 1H); ^{13}C NMR (CD_3OD) δ 61.4, 68.8, 83.7, 91.9, 92.6, 93.7, 111.1, 113.0,128.1, 161.7; ^{19}F NMR (CD_3OD) δ − 195.5 (ddd, J = 54.9, 25.0, 19.8 Hz); HRMS (ESI) for $C_{10}H_{10}N_3O_5FNa$ (MNa^+), calculated: 294.0506; observed: 294.0496.

6-Amido-2′-deoxy-2′-fluoro-β-D-uridine (30): Compound **24** was deprotected to yield product **30** as a white solid (212 mg, 61% yield). UV λ_{max} (MeOH) = 264 nm (ε 2,655 $mol^{-1}cm^{-1}$). ^1H NMR (CD_3OD) δ 3.68 (dd, 1H), 3.79–3.88 (m, 2H), 4.49 (ddd, 1H, H-3′, J_{H-F} =19 Hz), 5.38 (ddd, 1H, H-2′, J_{H-F} =56 Hz), 5.73 (dd, 1H, H-1′, J_{H-F} =26 Hz), 5.81(s, 1H); ^{13}C NMR (CD_3OD) δ 61.9, 69.0, 83.7, 92.0, 94.5, 101.7, 150.3, 150.5, 164.0, 164.7; ^{19}F NMR (CD_3OD) δ − 195.2 (ddd, J = 55.5, 25.8, 19.0 Hz); HRMS (ESI) for $C_{10}H_{12}N_3O_6FNa$ (MNa^+), calculated: 312.0589; observed: 312.0602.

5-Cyano-2′-deoxy-2′-fluoro-β-D-uridine (31): Product **31** was obtained as a yellow solid (532 mg, 87% yield) from compound **26**. UV λ_{max} (MeOH) = 274 nm (ε 4066 $mol^{-1}cm^{-1}$); ^1H NMR (CD_3OD) δ 3.79 (dd, 1H), 3.99–4.09 (m, 2H), 4.23 (ddd, 1H, H-3′, J_{H-F}=24 Hz), 5.0 (dd, 1H, H-2′, J_{H-F}=53 Hz), 5.95 (d, 1H, H-1′, J_{H-F}=16 Hz), 9.0 (s, 1H, H-6); ^{13}C NMR δ 58.7, 67.1, 83.9, 89.0, 92.7, 95.2, 113.4, 149.39, 149.6, 160.9; ^{19}F NMR (CD_3OD) δ 145.3 (ddd, J =52.1, 23.2, 16.0); HRMS (ESI) for $C_{10}H_{11}N_3O_5F$ (MH^+), calculated: 272.0666; observed: 272.0677.

2′-Deoxy-2′-fluoro-β-D-orotidine ethyl ester (32): Compound **21** was deprotected to yield compound **32** as a white solid (93 mg, 81% yield). UV λ_{max} (MeOH) = 272 nm (ε 2887 $mol^{-1}cm^{-1}$). ^{1}H NMR (CD_3OD) δ 1.36 (t, 3H), 3.62–3.69 (m, 1H), 3.80–3.84 (m, 2H), 4.35–4.48 (m, 3H), 5.34 (ddd, 1H, H-2′, J_{H-F} = 55 Hz), 5.85 (dd, 1H, H-1′, J_{H-F} =25 Hz), 6.07 (s, 1H); ^{19}F NMR (CD_3OD) δ − 195.54 (ddd, J = 55.4, 25.5, 19.1 Hz); HRMS (ESI) for $C_{12}H_{15}N_2O_7FNa$ (MNa^+), calculated: 341.0756; observed: 341.0755.

2′-Deoxy-2′-fluoro-6-iodo-β-D-uridine-5′-*O*-monophosphate (33): Compound **27** (100 mg, 0.27 mmol) was added to a solution of water (14 μL, 0.78 mmol), CH_3CN (2.5 mL), pyridine (0.1 mL, 1.28 mmol), and $POCl_3$ (164 mg, 0.1 mL, 1.1 mmol) at 0°C. The reaction mixture was stirred for 5 h at 0°C. The reaction was quenched with cold water (2 mL), concentrated, and the crude product was purified by Dowex (H^+) resin using 100% water followed by 5% formic acid as an eluent. The product was then dissolved in 3 mL of cold water, neutralized to pH 7 with a saturated NH_4OH solution, and lyophilized to obtain compound **33** as a white solid (54 mg, 41% yield). UV λ_{max} (MeOH) =267 (ε 948 $mol^{-1}cm^{-1}$); $^{1}HNMR$ (D_2O) δ 3.89 (dd, 1H), 4.02 (m, 2H), 4.65 (m, 1H), 5.51 (dd, 1H, H-2′, J_{H-F}=57 Hz), 6.08 (s, 1H), 6.26 (d, 1H, H-1′, J_{H-F}=30 Hz). ^{31}P NMR (D_2O) δ 1.04 (s); HRMS (ESI) calculated for $C_9H_{10}N_2O_8P$ (M^-): 305.0180; observed: 305.0191.

6-Azido-2′-deoxy-2′-fluoro-β-D-uridine-5′-*O*-monophosphate (34): A procedure similar to that for compound **33** was used. The reaction was carried out in the dark, and product **34** was obtained as a white solid (23 mg, 37% yield) from compound **28**. UV λ_{max}(MeOH) =283 nm (ε 9,179 $mol^{-1}cm^{-1}$); ^{1}H NMR (D_2O) δ 4.00 (m, 2 H), 4.14 (m, 1 H), 4.62 (ddd, 1H, H-3′, J_{H-F}=20.6 Hz), 5.44 (dd, 1H, H-2′, J_{H-F}=55 Hz), 5.69 (s, 1H), 6.18 (dd, 1H, H-1′, J_{H-F}=27.5 Hz),. ^{19}F NMR (D_2O) δ − 192.2 (ddd, J_{H-F}=55, 20.7, 25.8 Hz). ^{31}P NMR (D_2O) δ 1.13 (s); HRMS (ESI) for $C_9H_{11}FN_5NaO_8P^+$ (M-2NH_4+Na+2H^+), calculated: 390.0227; observed: 390.0226.

6-Cyano-2′-deoxy-2′-fluoro-β-D-uridine-5′-*O*-monophosphate (35): Compound **29** (154 mg, 0.6 mmol) was added to a stirred solution of $POCl_3$ (0.2 mL, 2.3 mmol), H_2O (0.03 mL, 1.6 mmol), CH_3CN (3 mL), and pyridine (0.2 mL, 2.7 mmol) at 0°C and stirred for 7 h. The reaction mixture was quenched with ice, concentrated, and the crude product was purified using a Biotage SP1™ column chromatography system (C18 column, 100% H_2O) and lyophilized to give **35** as a white foam (83 mg, 38% yield). UV λ_{max} (H_2O) =278 nm (ε 2,793 $mol^{-1}cm^{-1}$); ^{1}H NMR (D_2O) δ 3.80–3.88 (m, 1H), 3.94–4.03 (m, 2H), 4.51 (ddd, 1H, H-3′, J_{H-F} =21 Hz), 5.40 (ddd, 1H, H-2′, J_{H-F} =55 Hz), 5.88 (dd, 1H, H-1′, J_{H-F}=26 Hz), 6.46 (s, 1H); ^{19}F NMR (D_2O) δ − 194.0 (ddd, J= 54.4, 25.3, 20.5 Hz); ^{31}P NMR (D_2O) δ 3.80 (s); HRMS (ESI) for $C_{10}H_{10}N_3O_8FP$ (M^-), calculated: 350.0207; observed: 350.0195.

6-Amido-2′-deoxy-2′-fluoro-β-D-uridine-5′-*O*-monophosphate (36): A procedure similar to that for compound **35** was used. The product was obtained as a white solid (70 mg, 31% yield) from compound **30**. UV λ_{max} (MeOH) = 264 nm (ε 2,414 $mol^{-1}cm^{-1}$); ^{1}H NMR (D_2O) δ 3.77–3.88 (m, 1H), 3.88–4.0 (m, 2H), 4.43 (ddd, 1H, H-3′, J_{H-F} =20 Hz), 5.35 (dd, 1H, H-2′, J_{H-F} =55 Hz), 5.65 (d, 1H, H1′, J_{H-F} =26 Hz), 5.94 (s, 1H), 8.31 (s, 1H); ^{19}F NMR (D_2O) δ −194.1 (ddd, J =55.1, 25.5, 20.2 Hz); ^{31}P NMR (D_2O) δ 3.94 (s); HRMS (ESI) for $C_{10}H_{12}N_3O_9FP$ (M^-), calculated: 368.0305; observed: 368.0300.

5-Cyano-2′-deoxy-2′-fluoro-β-D-uridine-5′-*O*-monophosphate (37): A stirred solution of $POCl_3$ (0.2 mL, 2.3 mmol) and H_2O (0.03 mL, 1.6 mmol) in CH_3CN (3 mL) was treated with pyridine (0.02mL, 2.7 mmol) at 0°C, **31** (150 mg, 0.57 mmol) was added, and the reaction mixture was stirred at 0°C for 7 h. The reaction mixture was quenched with cold water and continuously stirred overnight at 22°C. Following evaporation of the solvent, the reaction mixture was brought to pH 6 with NH_4OH, purified on a Biotage SP1™

chromatography system (C18, mobile phase: 100% H_2O), concentrated, and lyophilized to obtain compound **37** as a solid (79 mg, 36% yield). UV λ_{max} (MeOH)=274 nm (ε 3412 $mol^{-1}cm^{-1}$); ^1H NMR (D_2O) δ 3.79 (dd, 1H), 3.97–4.16 (m, 2H), 4.23 (ddd, 1H, H-3′, J_{H-F}=23 Hz), 5.0 (dd, 1H, H-2′, J_{H-F}=53 Hz), 5.86 (d, 1H, H-1′, J_{H-F}=19 Hz), 8.3 (s, 1H, H6); ^{19}F NMR (D_2O) δ 148.6 (ddd, *J*=52.8, 23.0, 18.8 Hz); ^{31}P (D_2O) δ 4.97 (s); HRMS (ESI) for $C_{10}H_{10}N_3O_8FP$ (M^-), calculated: 350.0190; observed: 350.0195.

6-Amino-2′-deoxy-2′-fluoro-β-D-uridine (38): Compound **28** (84 mg, 0.29 mmol) was dissolved in 50% aqueous MeOH (6 mL) in the dark and was treated with 10% Pd/C (9 mg). The reaction mixture was stirred for 3 h under a hydrogen atmosphere at 1 atm at room temperature and filtered through a pad of Celite™. The solvent was evaporated under vacuum to yield compound **38** (59 mg, 78% yield) as a pale yellow solid. UV λ_{max} (MeOH)=270 nm (ε 17,147 $mol^{-1}cm^{-1}$); ^1H NMR (D_2O) δ 3.74 (dd, 1H), 3.90 (dd, 1H), 3.97 (m, 1H), 4.51 (ddd, 1H, H-3′, J_{H-F}=18.3 Hz), 4.93 (s, 1H), 5.46 (dd, 1H, H-2′, J_{H-F}=54.4 Hz), 5.94 (dd, 1H, H-1′, J_{H-F}=25.8 Hz),. ^{19}F NMR (D_2O) δ −193.68 (ddd, *J*=54.4, 18.3, 25.8 Hz). HRMS (ESI) for $C_9H_{13}FN_3O_5$ (MH+), calculated: 262.0840, observed: 262.0841; for $C_9H_{12}FN_3NaO_5$ (MNa+), calculated: 282.0659, observed: 284.0659.

Enzymology: Assays were performed on a VP-ITC microcalorimeter (MicroCal/GE Healthcare) using established protocols.[15,20] *Mt* ODCase was used as a model enzyme, and assays with human ODCase were conducted when possible.

Reversible, competitive inhibition of ODCases—Concentrated enzyme stock solutions were prepared in 50 mM Tris, pH 7.5, 20 mM DTT, and 40 mM NaCl. Concentrated stocks of the substrate, OMP, and inhibitors were prepared in 50 mM Tris. The stock concentration of *Mt* ODCase was 20 μM and that of human ODCase was 60 μM. The assay temperatures for the human and *Mt* enzymes were 37 and 55°C, respectively. The final concentration of *Mt* ODCase in the control reaction was 20 nM, and the final substrate concentration was 40 μM. The final concentration of human ODCase was 60 nM in the assay mixture, and the final concentration of the substrate was 20 μM.

Time-dependent inactivation of human and Mt ODCases—Enzyme stocks (70 and 25 μM for human and *Mt*, respectively) were prepared in 50 mM Tris, pH 7.5, 20 mM DTT, and 40 mM NaCl and were incubated overnight at room temperature prior to evaluation using the assay. The substrate and the inhibitor were prepared in 50 mM Tris buffer. Assay samples were prepared in a degassed buffer (50 mM Tris, 1 mM DTT, pH 7.5).

Human enzyme (60 μM) or *Mt* ODCase was incubated at room temperature in the presence of inhibitor **33** at various concentrations. Aliquots of 2.5 μL of the incubation mixture were diluted to a final volume of 2.5 mL in 50 mM Tris and 1 mM DTT buffer. The remaining enzyme activity was then measured by introducing 5 mM substrate (5.7 and 11.4 μL for human and *Mt* ODCases, respectively) via a single injection into the sample cell of the calorimeter. Samples containing 20 μM enzyme and compound **35** at various concentrations were incubated at room temperature for up to 48 h. The control reaction contained no inhibitor. For the time-dependent assay using the 6-azido derivative **34** against *Mt* ODCase, the enzyme (20 μM) was incubated at room temperature in the presence of various concentrations of **34**. The remaining enzyme activity was measured in the control and inhibitor-treated samples at various time points.

Mass spectral analyses—Mass spectra for the enzymes and the complexes were obtained at the Mass Spectrometry-AIMS Laboratory, Department of Chemistry, University of Toronto on a AB/Sciex QStar mass spectrometer with an electrospray ionization (ESI)

source and on an Agilent 1100 capillary LC (MDS Sciex). All samples were prepared in 50 mM Tris (pH 7.5), 20 mM DTT, and 40 mM NaCl. Human ODCase was exposed to 29 mM **34**, and *Mt* ODCase was incubated in the presence of 25 mM **34** overnight at room temperature in the dark. The reaction mixture of human ODCase and **33** was measured after 2 h of incubation of the enzyme (60 μM) with the inhibitor (3 mM).

For compound **35**, the inhibitor was incubated overnight with either human or *Mt* ODCase. The concentrations of the human ODCase and compound **35** were 100 μM and 437.5 mM, and those for *Mt* ODCase and **36** were 200 μM and 388 mM, respectively.

Data analyses—The raw data were analyzed using Origin 7.0 software. First, the data were adjusted for the time delay (16 sec) for the start of the reaction in the isothermal calorimeter (ITC), and the baseline was adjusted using the "baseline" function. These data were then converted into rate versus [*S*] plots. All data sets were fitted to equation 1:

$$v=\frac{V_{\max}[S]}{K_M+[S]} \qquad \text{Equation 1}$$

The data sets were further analyzed using Grafit 5.0 to derive the inhibition parameters for competitive inhibitors. The inhibition constant, K_i, for reversible (competitive) inhibition was determined by fitting the rate versus [*S*] data to equation 2:

$$v=\frac{V_{\max}[S]}{K_M\left(1+\frac{[I]}{K_i}\right)+[S]} \qquad \text{Equation 2}$$

To determine the inactivation parameters for the inhibition of human and *Mt* ODCases by 6-iodo derivative **34**, k_{obs} was first computed at each inhibitor concentration from the slope of ln(% remaining enzyme activity) versus time. The calculated k_{obs} and the inhibitor concentrations [*I*] were used to calculate the second-order rate constant of inactivation (k_{obs}/[*I*]). The inactivation of *Mt* ODCase due to inhibitors **35** and **36** followed first-order reaction kinetics. The K_I and k_{ianct} were derived for each inhibitor from the nonlinear least squares fit of the k_{obs} versus the inhibitor concentration to the following equation:

$$k_{obs}=\frac{k_{inact}[I]}{K_I+[I]} \qquad \text{Equation 3}$$

X-Ray Crystallography

Crystallization and collection of diffraction data—All human ODCase concentrations were determined using a BioRAD protein assay kit and bovine serum albumin (BSA) as a standard. Crystals were grown at room temperature using the hanging-drop method; 2 μL of protein solution containing 10 mg/mL enzyme, 10 mM 6-iodo derivative **33** in 25 mM HEPES pH 7.5, 500 mM NaCl, 5% glycerol, and 25 mM EDTA, were mixed with 2 μL of the respective reservoir solution. Preliminary hits were optimized. For data collection, the crystals were cryo-protected by bringing the mother liquor to 20% glycerol before flash-freezing in a stream of boiling nitrogen. Diffraction data were collected at 100 K and λ = 0.97934 Å on beamline 08ID-1 at the Canadian Macromolecular Crystallography Facility at the Canadian Light Source, Inc. Data were reduced and scaled using HKL2000.[32]

The structure of the enzyme complex was determined using molecular replacement techniques with the program package MOLREP; subsequent refinement was performed with Refmac-5.2, and model building used COOT.[33,34,35] Statistics for data collection and refinement are given in Table 3. Atomic coordinates and structure factors have been deposited into the Protein Data Bank (PDB IDs: ****).

Results and Discussion

Nucleosides with modified carbohydrates carrying fluoro and difluoro substitutions have shown potent antiviral and anticancer activities.[36,37] This is due to the structural and conformational influences introduced by the fluoro moiety onto the carbohydrate moiety of the nucleosides as well as the improved metabolic stabilities of such modified nucleosides.[24,38,39,40] Incorporation of the fluorine moiety at the 2′-position of the ribofuranosyl uridine derivatives is based on the idea that a fluorine atom (radius of 1.47 Å) could mimic the features of an oxygen or a hydrogen atom (radii of 1.52 and 1.20 Å, respectively). Despite a long history of incorporation of fluorines onto carbohydrate moieties and nucleosides, there are no general principles linking the substitution of fluorines onto nucleosides and the potential improvements in the corresponding biological activities, specifically in relation to their binding to the target site. To investigate the effect of the 2′-fluoro moiety on the binding of ligands to ODCase, we synthesized a series of nucleoside derivatives in which the 2′-hydroxyl moiety was substituted with a fluorine atom in addition to the substitutions at the C-5 or C-6 positions of the uridine moiety (Figure 2).

The target compounds were synthesized from the key intermediate **18** (Scheme 1).[31] First, the arabinosyl moiety in compound **18** was transformed into the 2′-fluoro ribosyl configuration by treatment with diethylamino sulfur trifluoride to yield the fluoro derivative **19**. This derivative was then treated with LDA followed by iodine or ethyl chloroformate to obtain compounds **20** and **21**, respectively.[41] Compound **22**, carrying a C5-bromo substitution, was obtained by the treatment of fully protected uridine **19** with *N*-bromosuccinimide. Compound **22** was then transformed into the 6-cyano derivative **23** exclusively by treatment with sodium cyanide at 22°C.[42]

The 6-cyano derivative **23** was treated with sodium hydroxide to obtain 6-amido derivative **24** (Scheme 1A). Treatment of 6-iodo derivative **20** with sodium azide yielded the 6-azido derivative **25** (Scheme 1B). The 5-cyano derivative **26** was obtained by the treatment of 5-bromo derivative **22** at 150°C for 5 min under microwave conditions using the modified procedure of Torrence et al. (Scheme 1C).[43] Compounds **20, 21**, and **23–26** were deprotected using Amberlite® (H^+), yielding the corresponding 6-substituted-2′-fluoro nucleosides **27–32** (Scheme 2A). These nucleosides were phosphorylated at the 5′-position to obtain the corresponding nucleotides **33–37**. 6-Amino uridine derivative **38** was obtained by the reduction of the corresponding azido derivative **28** (Schemes 2B).

First, 6-cyano derivative **35** was investigated as a reversible inhibitor of ODCase (**35** is also a time-dependent inactivator of ODCase, and its characteristics are presented after this discussion). Compound **35** exhibited moderate inhibition of *Mt* ODCase as a competitive inhibitor with an inhibition constant (K_i) of 37.0 ± 2.5 μM, but it did not inhibit the catalytic activity of human ODCase up to a concentration of 2 mM (Table 1). In comparison, 6-cyano ribosyl derivative **11** is a moderate inhibitor of *Mt* ODCase with an inhibition constant of K_i = 29 μM.[16] The 6-amido-2′-deoxy-2′-fluoro analog **36** was a poor inhibitor of both human and *Mt* ODCases (K_i >3 mM) (Table 1). Compound **37**, carrying a cyano group at C5 position, exhibited weaker inhibition of the catalytic activity of ODCase (K_i = 360 ± 23 and 759 ± 88 μM, against *Mt* and human ODCases, respectively; Table 1). 6-Amido-UMP, a close analog of the substrate OMP, and its 2′-deoxy-2′-fluoro analog **36** were poor inhibitors

of *Mt* ODCase, with K_is of 1.32 ± 0.04 and 3.32 ± 0.18 mM, respectively. In general, competitive inhibition of ODCases by 2′-deoxy-2′-fluoro uridine derivatives was either similar to or weaker than the corresponding ribosyl derivatives.[16,17,21] Compounds with 2′-fluoro substitution did not necessarily improve the potency of the synthesized nucleotides against ODCase as competitive inhibitors. At the outset, the loss of potency by one or more folds in the 2′-fluorinated nucleotides may have been due to the loss of hydrogen-bonding interactions when the 2′-hydroxyl moiety was replaced with the fluorine atom. However, there were other significant reactivities that were introduced onto the 2′-fluorinated nucleotides (*vide infra*), despite the loss of hydrogen-bonding strength. Among the 2′-fluorinated derivatives, the inhibitory constants (K_is) against the human and *Mt* ODCases varied up to 3 orders of magnitude (Table 1). Such variations were due to differences in the species that existed between the *Mt* and human ODCases and are commonly seen with other classes of inhibitors.[20]

Three of the derivatives, **33**, **34**, and **35**, carrying the iodo, azido, and cyano moieties, respectively, at the C6 position of the nucleotide exhibited time-dependent inactivation of ODCases, which was discovered during the enzyme kinetics experiments. While compounds **33** and **34** were expected to behave as covalent and time-dependent inhibitors, compound **35**, carrying a 6-cyano moiety, displayed surprising behavior; it inactivated ODCase irreversibly, forming a covalent bond. 6-Iodo derivative **33** inactivated human ODCase irreversibly with a second-order rate constant (K_{obs}/[I]) of 2.0 ± 0.01 $M^{-1}sec^{-1}$ and with a three-fold increase in the rate of inactivation against *Mt* ODCase (0.62 ± 0.02 $M^{-1}sec^{-1}$) (Table 2). 6-Azido derivative **34** and 6-cyano derivative **35** were weaker inactivators, with equilibrium inhibition constants (K_I) of 1.2 ± 0.1 and 30 ± 6 mM, respectively, against *Mt* ODCase (Table 2). The first-order rates of inactivation (k_{inact}) were 4.0 ± 0.2 h^{-1} for **34** and 2.0 ± 0.2 h^{-1} for compound **35**. Interestingly, 6-azido-5-fluoro-UMP (**12**) exhibited higher affinity (K_I) than the corresponding 2′-deoxy-2′-fluoro derivative **34**. In comparison, 6-azido-UMP (**14**) was a potent compound, with an equilibrium inhibition constant of K_I = 6.3 ± 1.1 × 10^{-4} mM, which was about 30-fold higher than that due to the 5-fluoro derivative **12** and about 2000-fold more potent than the corresponding 2′-deoxy-2′-fluoro derivative **34** (Table 2). The ribofuranosyl analog, 6-iodo-UMP (**10**), was the most potent of all these molecules, with a second-order rate constant ~5 orders of magnitude higher than that of the corresponding 2′-deoxy-2′-fluoro analog **33** (k_{inact} =2.6 × 10^5 h^{-1}).

The irreversible inhibitors of ODCase, **33–35**, were further analyzed to confirm the covalent binding to the enzyme. Thus, the ODCase enzyme was incubated with each inhibitor, and the sample was analyzed using mass spectrometry. Compounds **33** and **34**, the 6-iodo and 6-azido derivatives, showed a covalent complex after elimination of the 6-substitution, as expected (data not shown). This pattern was very similar to the corresponding 6-substituted UMP derivatives.[15,16,17] However, compound **35**, carrying a 6-cyano moiety, surprisingly produced a covalent complex; the mass implied that the mechanism for the time-dependent loss of activity was due to covalent bond formation (Figure 6A). In the control experiment, the mass for the enzyme was clearly seen at 27,344 a.m.u. (inset in Figure 6A). When the enzyme-ligand complex with **35** was analyzed, along with the native ODCase at 27,344 a.m.u., an additional and significant peak at 27,668 a.m.u. was observed, corresponding to the molecular weight of the enzyme and **33** after removal of the cyano group. This unequivocally confirmed covalent bond formation between the enzyme and ligand when ODCase was challenged with **33**. This process was slow, as seen in the enzyme kinetics, with a k_{inact} of 4.0 ± 0.2 h^{-1}. This was unexpected because none of the other 6-cyano-UMP derivatives showed a covalent complex with ODCase, but they exhibited other unnatural biochemical transformations in the presence of ODCase. For example, 6-CN-UMP (**11**) in the presence of ODCase was transformed into 6-hydroxy-UMP or BMP (**3**), a chemically unknown transformation.[22,23] There was no evidence for covalent bond formation in the

case of **11** with the wild-type ODCase, but a hydrolysis (of C6–C7 bond) facilitated by ODCase leading to **3** occurred (Figure 6B). Substitution of the 2′-hydroxyl moiety with a fluorine moiety probably influenced the microenvironment and nucleophilicity of the active site residue, Lys72 (*Mt* ODCase numbering, equivalent to Lys125 residue in human ODCase), upon binding of ligand **35** to the active site of ODCase. Instead of a water molecule, as seen for **11**, Lys72 displaced the C6 cyano group, leading to covalent bond formation similar to those of 6-iodo and 6-azido derivatives **33** and **34**. These experiments were repeated using human ODCase, and results identical to those of *Mt* ODCase were observed.

6-Iodo derivative **33** was co-crystallized with the human ODCase, and its three-dimensional structure was determined to understand the interactions of this class of compounds with the catalytic site of ODCase (Figure 4A). 2′-Fluoro-6-iodo-UMP (**33**) assumed a similar conformation, and a similar hydrogen-bonding network was formed, except at the 2′ position of the ribosyl moiety, when compared with the complex of its ribosyl derivative **10** (Figures 4A vs 4B). This is the first time that a 2′-fluoronucleotide was co-crystallized with a biological target. Gonin et al. reported the three-dimensional structure of the complex of a nucleoside diphosphate kinase (NDK) with a 2′,3′-dideoxy-3′-fluoro nucleotide, which was the only other fluororibosyl nucleotide co-crystallized with its target enzyme (Figure 4C).[44] The substitution of the 3′-hydroxyl moiety in 2′-deoxy-UDP with a fluorine atom led to the loss of catalytic efficiency of NDK.[44] However, 2′,3′-dideoxy-UDP, lacking the 3′-fluoro moiety, was a better substrate to NDK than the fluorinated analog.

In the co-crystal structure of **33** bound to ODCase, a covalent bond was observed between the C6 of **33** and Lys-125 in the active site of human ODCase (Figure 4A). Two strong hydrogen bonds with the residues Asp128 and Thr132 in the active site of ODCase were compromised in the case of **33** due to the weaker hydrogen bonding potential of fluorine as well as unfavorable interactions (Figure 5). An unfavorable interaction of the carboxyl moiety of Asp128 and the 2′-fluoro moiety was observed in the complex between **33** and ODCase, leading to hydrogen-bonding interactions between Asp128 and Lys125- N_{ε}. Such an interaction was absent in the co-crystal structure with **10** because the 2′-hydroxyl moiety was occupied by Asp128 via a classical hydrogen bond.

The 2′-fluoro-6-substituted uridine derivatives were evaluated for their antimalarial and anticancer activities. None of the synthesized nucleosides exhibited significant antimalarial activities against *Plasmodium falciparum* (3D7) or any significant anticancer activities in OCI-AML-1 cell lines (acute myeloid leukemia) in the cell-based assays (Table 4). Although the inhibition constants against the isolated enzyme ODCase revealed reasonable potency for the 2′-fluoro-6-substituted mononucleotide derivatives, the lack of cellular activities may have been due to the poor activation of these modified nucleosides into the corresponding mononucleotide forms. It is also interesting to note that 2′-fluoro-2′-deoxyuridine possessing a 5-(2-iodovinyl) substituent and 2′-deoxy-2′-fluoro-5-iodouridine undergo very low uptake in normal cells, but very high uptake in thymidine kinase postive cells.[45] Both compounds exhibit weak antiviral activities. This suggests a 2′-ribo-2′-deoxyuridine moiety should be considered carefully for potential cellular and *in vivo* therapeutic activities.

In summary, we determined the structure-activity relationships of 2′-deoxy-2′-fluoro-UMP derivatives as potential ODCase inhibitors and revealed novel chemistry of these fluorinated nucleotides with the target enzyme. While these nucleosides do meet the general criteria defined for the ODCase pharmacophore,[14] issues of species of origin of the specific ODCase and the activation of the fluorinated nucleosides into the corresponding mononucleotides affect their ultimate therapeutic activities. The influence of 2′-fluoro moiety on modulation

of the reactivity at the C6 center of the nucleotide could be used in the design of novel inhibitors of ODCase and perhaps other enzymes that accept nucleotides as ligands.

Supplementary Material

Refer to Web version on PubMed Central for supplementary material.

Acknowledgments

The authors thank Mr. Terence To for help with the expression and purification of ODCase enzymes. This work was supported by the Canadian Institutes of Health Research (EFP & LPK) and University Health Network. LPK, EFP, KCK and IC thank the financial support from ISTPCanada. EFP acknowledges support through the Canada Research Chairs program. We thank the staff at BioCARS, sector 14 beamlines, at the Advanced Photon Source, Argonne National Laboratories, for their generous time commitment and support. Use of the Advanced Photon Source was supported by the Basic Energy Sciences, Office of Science, United States Department of Energy, under contract W-31-109-Eng-38. Use of the BioCARS sector 14 was supported by the National Center for Research Resources, National Institutes of Health, under grant RR07707. We also gratefully acknowledge the help we received from the staff of the Canadian Macromolecular Crystallography Facility at the Canadian Light Source, which is supported by NSERC, NRC, CIHR, and the University of Saskatchewan.

Abbreviations

Mt	*Methanobacterium thermoautotrophicum*
ODCase	Orotidine-5′-monophosphate decarboxylase
UMP	Uridine-5′-monophosphate
OMP	Orotidine-5′-monophosphate
ITC	Isothermal calorimeter
BMP	Barbiturate-5′-monophosphate

References

1. Cui W, DeWitt JG, Miller SM, Wu W. No metal cofactor in orotidine 5′-monophosphate decarboxylase. Biochem Biophys Res Comm. 1999; 259:133–135. [PubMed: 10334928]
2. Shostak K, Jones ME. Orotidylate decarboxylase: insights into the catalytic mechanism from substrate specificity studies. Biochemistry. 1992; 31:12155–12161. [PubMed: 1457411]
3. Reichard P. The enzymic synthesis of pyrimidines. Adv Enzymol Mol Biol. 1959; 21:263–294.
4. Donovan WP, Kushner SR. Purification and characterization of orotidine-5′-phosphate decarboxylase from Escherichia coli K-12. J Bacteriol. 1983; 156:620–624. [PubMed: 6355062]
5. Pragobpol S, Gero AM, Lee CS, O'Sullivan WJ. Orotate phosphoribosyltransferase and orotidylate decarboxylase from *Crithidia luciliae*: subcellular location of the enzymes and a study of substrate channeling. Arch Biochem Biophys. 1984; 230:285–293. [PubMed: 6712237]
6. Gero AM, O'Sullivan WJ. Purines and pyrimidines in malarial parasites. Blood Cells. 1990; 16:485–498.
7. Reyes P, Guganig ME. Studies on a pyrimidine phosphoribosyltransferase from murine leukemia P1534J. Partial purification, substrate specificity, and evidence for its existence as a bifunctional complex with orotidine 5-phosphate decarboxylase. J Biol Chem. 1975; 250:5097–5108. [PubMed: 1171096]
8. McClard RW, Black MJ, Livingstone LR, Jones ME. Isolation and initial characterization of the single polypeptide that synthesizes uridine 5′-monophosphate from orotate in Ehrlich ascites carcinoma. Purification by tandem affinity chromatography of uridine-5′-monophosphate synthase. Biochemistry. 1980; 19:4699–4706. [PubMed: 6893554]

9. Meza-Avina ME, Wei L, Buhendwa MG, Poduch E, Bello AM, Pai EF, Kotra LP. Inhibition of orotidine 5′-monophosphate decarboxylase and its therapeutic potential. Mini-Rev Med Chem. 2008; 8:239–247. [PubMed: 18336344]
10. Levine HL, Brody RS, Westheimer FH. Inhibition of orotidine-5′ phosphate decarboxylase by 1-(5′-phospho-®-D-ribofuranosyl)barbituric acid, 6-azauridine-5′-phosphate, and uridine 5′-phosphate. Biochemistry. 1980; 19:4993–4999. [PubMed: 7006681]
11. Scott HV, Gero AM, O'Sullivan WJ. In vitro inhibition of Plasmodium falciparum by Pyrazofurin, an inhibitor of pyridine biosynthesis de novo. Mol Biochem Parasitol. 1986; 18:3–15. [PubMed: 3515174]
12. Christopherson RI, Lyons SD, Wilson PK. Inhibitors of de novo nucleotide biosynthesis as drugs. Acc Chem Res. 2002; 35:961–971. [PubMed: 12437321]
13. Najarian T, Traut TW. Nifedipine and nimodipine competitively inhibit uridine kinase and orotidine-phosphate decarboxylase: theoretical relevance to poor outcome in stroke. Neurorehabil Neural Repair. 2000; 14:237–2341. [PubMed: 11272481]
14. Meza-Avina, ME.; Wei, L.; Liu, Y.; Poduch, E.; Bello, AM.; Mishra, RK.; Pai, EF.; Kotra, LP. Structural determinants for inhibitory ligands of orotidine-5′-monophosphate decarboxylase. Bioorg Med Chem. 2010. in press. (http://dx.doi.org/10.1016/j.bmc.2010.04.017)
15. Poduch E, Bello AM, Tang S, Fujihashi M, Pai EF, Kotra LP. Design of inhibitors of orotidine monophosphate decarboxylase using bioisosteric replacement and determination of inhibition kinetics. J Med Chem. 2006; 49:4937–4945. [PubMed: 16884305]
16. Bello AM, Poduch E, Liu Y, Wei L, Crandall I, Wang X, Dyanand C, Kain KC, Pai EF, Kotra LP. Structure-activity relationships of c6-uridine derivatives targeting *plasmodia* orotidine monophosphate decarboxylase. J Med Chem. 2008; 51:439–448. [PubMed: 18189347]
17. Bello AM, Konforte D, Poduch E, Furlonger C, Wei L, Lewis M, Pai EF, Paige CJ, Kotra LP. Structure-activity relationships of orotidine-5′-monophosphate decarboxylase inhibitors as anticancer agents. J Med Chem. 2009; 52:1648–1658. [PubMed: 19260677]
18. Crowther GJ, Napuli AJ, Gilligan JH, Gagaring K, Borboa R, Francek C, Chen Z, Dagostino EF, Stockmyer JB, Wang Y, et al. Identification of inhibitors for putative malaria drug targets among novel antimalarial compounds. Mol Biochem Parasitol. 2011; 175:21–29. [PubMed: 20813141]
19. Wittmann JG, Heinrich D, Gasow K, Frey A, Diederichsen U, Rudolph MG. Structures of the human orotidine-5′-monophosphate decarboxylase support a covalent mechanism and provide a framework for drug design. Structure. 2008; 16:82–92. [PubMed: 18184586]
20. Poduch E, Wei L, Pai EF, Kotra LP. Structural diversity and plasticity associated with nucleotides targeting orotidine monophosphate decarboxylase. J Med Chem. 2008; 51(3):432–438. [PubMed: 18181562]
21. Bello AM, Poduch E, Fujihashi M, Amani M, Li Y, Crandall I, Hui R, Lee PI, Kain KC, Pai EF, Kotra LP. A potent covalent inhibitor of orotidine 5′-monophosphate decarboxylase with antimalarial activity. J Med Chem. 2007; 50:915–921. [PubMed: 17290979]
22. Fujihashi M, Bello AM, Poduch E, Wei L, Annedi SC, Pai EF, Kotra LP. An unprecedented twist to odcase catalytic activity. J Am Chem Soc. 2005; 127:15048–15050. [PubMed: 16248642]
23. Fujihashi M, Wei L, Kotra LP, Pai EF. Structural characterization of the molecular events during a slow substrate-product transition in Orotinde-5′-monophosphate decarboxylase. J Mol Biol. 2009; 387:1199–1210. [PubMed: 19236876]
24. Pankiewicz KW. Fluorinated nucleosides. Carbohydrate Res. 2000; 327:87–105.
25. Isanbor C, O'Hagan D. Fluorine in medicinal chemistry: A review of anti-cancer agents. J Fluorine Chem. 2006; 127:303–319.
26. Begue JP, Bonnet-Delpon D. Recent advances (1995–2005) in fluorinated pharmaceuticals based on natural-products. J Fluorine Chem. 2006; 127:992–1012.
27. Meng W-D, Qing F-L. Fluorinated nucleosides as antiviral and antitumor agents. Curr Top Med Chem. 2006; 6:1499–1528. [PubMed: 16918465]
28. Barton-Burke M. Gemcitabine: a pharmacologic and clinical overview. Cancer Nurs. 1999; 22:176–183. [PubMed: 10217035]

29. Jeong LS, Tosh DK, Choi WJ, Lee SK, Kang YJ, Choi S, Lee JH, Lee H, Lee HW, Kim HO. Discovery of a new template for anticancer agents: 2′-deoxy-2′-fluoro-4′-selenoarabinofuranosyl-cytosine (2′-F-4′-seleno-ara-C). J Med Chme. 2009; 52:5303–5306.
30. Asselah T, Lada O, Moucari R, Marcellin P. Clevudine: a promising therapy for the treatment of chronic hepatitis B. Expert Opin Investig Drugs. 2008; 17:1963–1974.
31. Shi J, Du J, Ma T, Pankiewicz KW, Patterson SE, Tharnish PM, McBrayer TR, Stuyver LJ, Otto MJ, Chu CK, Schinazi RF, Watanabe KA. Synthesis and anti-viral activity of a series of D- and L-2′-deoxy-fluororibonucleosides in the subgenomic HCV replicon system. Bioorg Med Chem. 2005; 13:1641–1652. [PubMed: 15698782]
32. Otwinowski Z, Minor W. Processing of X-ray diffraction data collected in oscillation mode. Methods Enzymol. 1997; 276:307–326.
33. Vagin A, Teplyakov A. MOLREP: an automated program for molecular replacement. J Appl Crystallogr. 1997; 30:1022–1025.
34. Murshudov GN, Vagin AA, Dodson EJ. Refinement of macromolecular structures by the maximum-likehood method. Acta Crystallogr, Sect D: Biol Crystallogr. 1997; 53:240–255. [PubMed: 15299926]
35. Emsley P, Cowtan K. Model building tools for molecular graphics. Acta Crystallogr, Sect D: Biol Crystallogr. 2004; D60:2126–2132. [PubMed: 15572765]
36. Van Rompay AR, Johansson M, Karlsson A. Substrate specificity and phosphorylation of antiviral and anticancer nucleoside analogues by human deoxyribonucleoside kinases and ribonucleoside kinases. Pharmacol Ther. 2003; 100:119–139. [PubMed: 14609716]
37. Tan X, Chu CK, Boudinot FD. Development and optimization of anti-HIV nucleoside analogs and prodrugs: A review of their cellular pharmacology, structure-activity relationships and pharmacokinetics. Adv Drug Delivery Rev. 1999; 39:117–151.
38. Plavec J, Koole LH, Sandstrom A, Chattopadhyaya J. Structural studies of anti-HIV 3′-α-fluorothymidine & 3′-α-azidothymidine by 500 MHz 1H NMR spectroscopy and molecular mechanics (MM2) calculations. Tetrahedron. 1991; 47:7363–7376.
39. Barchi JJ Jr, Jeong LS, Siddiqui MA, Marquez VE. Conformational analysis of the complete series of 2′ and 3′ monofluorinated dideoxyuridines. J Biochem Biophys Methods. 1997; 34:11–29. [PubMed: 9089381]
40. Mikhailopulo I, Pricota TI, Sivets GG, Altona C. 2′-Chloro-2′,3′-dideoxy-3′-fluoro-D-ribonucleosides: Synthesis, stereospecificity, some chemical transformations, and conformational analysis. J Org Chem. 2003; 68:5897–5908. [PubMed: 12868924]
41. Shimuzu M, Tanaka H, Hayakawa H, Miyasaka T. Dynamic aspects in the LDA lithiathion of an arabinofuranosyl derivative of 4-ethoxy-2-pyrimidinone: Regioselective entry to both C-5 and C-6 substitutions. Tetrahedron Lett. 1990; 31:1295–1298.
42. Ueda T, Inoue H, Matsuda A. Synthesis and reaction of some 6-substituted pyrimidine nucleosides. Ann NY Acad Sci. 1975; 255:121–130. [PubMed: 1059349]
43. Torrence PF, Bhooshan B, Descamps J, De Clercq E. Improved synthesis and in vitro antiviral activities of 5-cyanouridine and 5-cyano-2′-deoxyuridine. J Med Chem. 1977; 20:974 – 976. [PubMed: 195058]
44. Gonin P, Xu Y, Milon L, Dabernat S, Morr M, Kumar R, Lacombe ML, Janin J, Lascu I. Catalytic mechanism of nucleoside diphosphate kinase investigated using nucleotide analogs, viscosity effects, and X-ray crystallography. Biochemistry. 1999; 38:7265–7272. [PubMed: 10353838]
45. Morin KW, Atrazheva ED, Knaus EE, Wiebe LI. Synthesis and cellular uptake of 2′-substituted analogs of (*E*)-5-(2-[125I]iodovinyl)-2′-deoxyuridine in tumor cells transduced with the herpes simplex type-1 thymidine kinase gene. Evaluation as probed for monitoring gene therapy. J Med Chem. 1997; 40:2184–2190. [PubMed: 9216837]

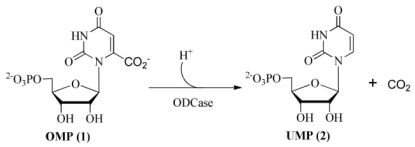

Figure 1.
Catalytic decarboxylation of OMP (**1**) to UMP (**2**) by ODCase for the synthesis of pyrimidine nucleotides in the *de novo* pathway.

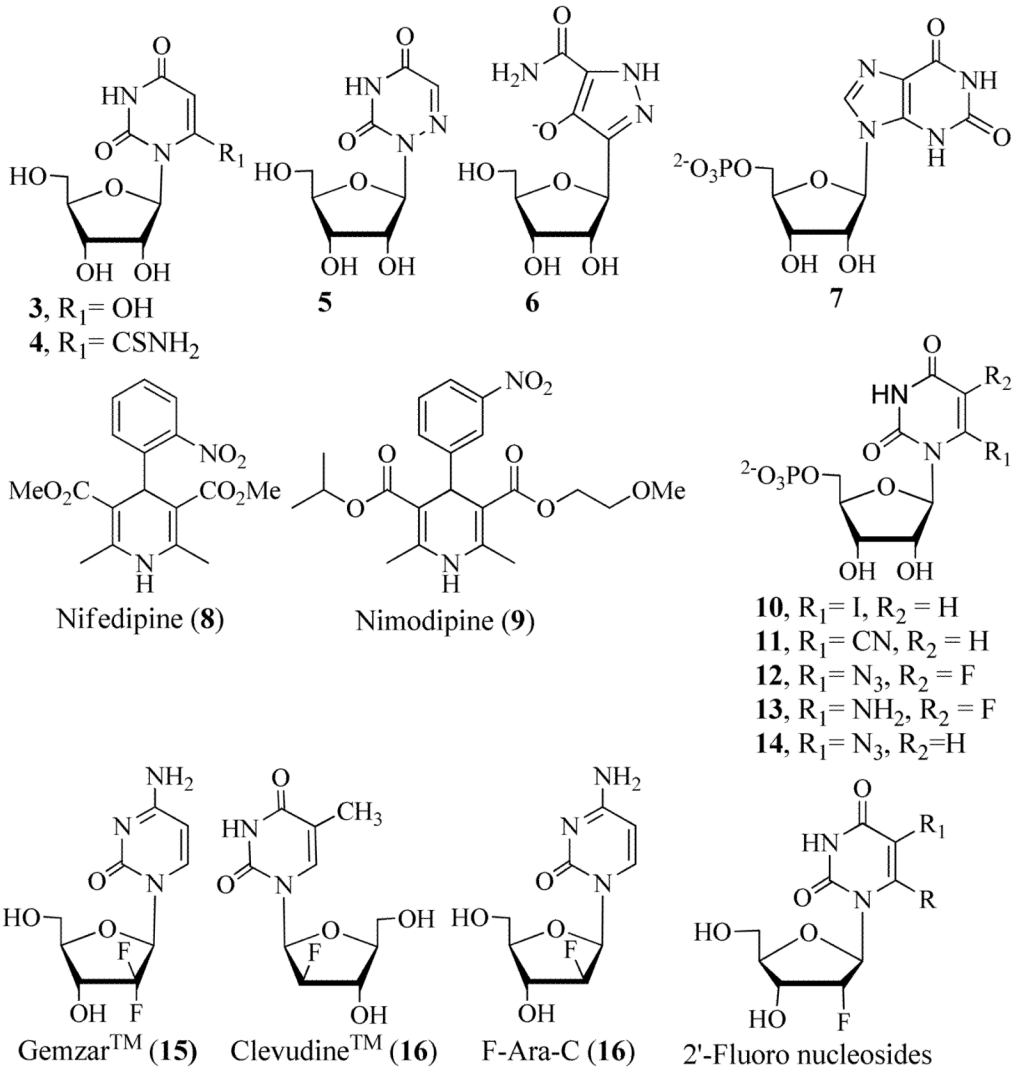

Figure 2.
Structures of various nucleosides and nucleotides with ODCase inhibitory properties.

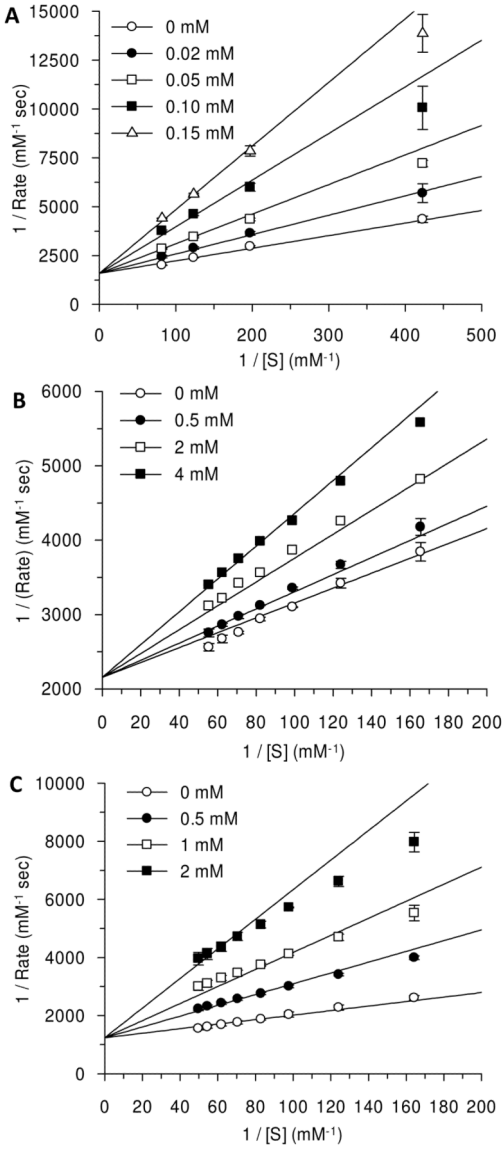

Figure 3.

Enzyme inhibition kinetics for 6-cyano derivative **35** (Panel A), 6-amido derivative **36** (Panel B), and 5-cyano derivative **37** (Panel C) against *Mt* ODCase.

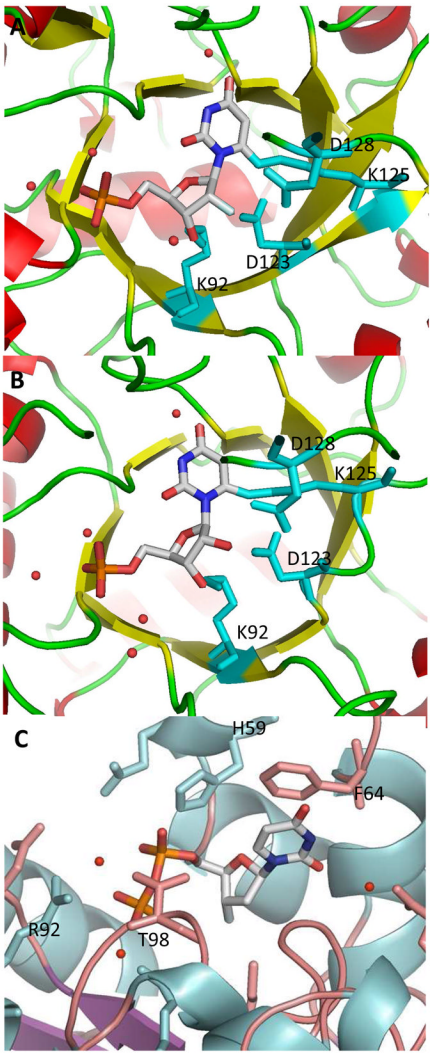

Figure 4.

(A) Co-crystal structure of human ODCase covalently modified by 2′-fluoro-6-iodo-UMP (**33**). (B) X-ray crystal structure of human ODCase covalently modified by 6-iodo-UMP (**10**) (pdb code: 3BGJ). (C) X-ray crystal structure of nucleoside diphosphate kinase bound by 3′-fluoro-UDP (pdb code: 1B99). Active site regions are shown with the ligand rendered according to atom type. The secondary structures of the proteins are shown, and only the important active site residues are shown in a capped stick representation. Water molecules are shown as red spheres.

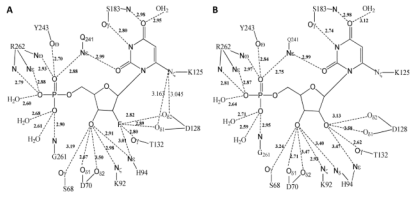

Figure 5.
Hydrogen-bonding networks of 2′-fluoro-6-iodo-UMP (**33**, Panel A) and of 6-iodo-UMP (**10**, Panel B) bound in the active site of human ODCase.

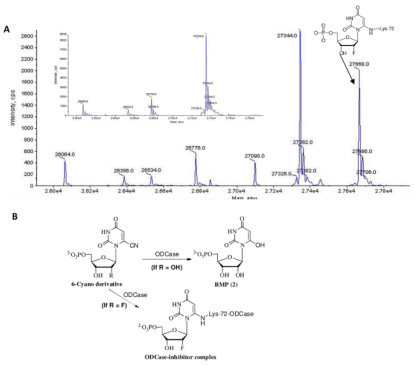

Figure 6.

(A) Mass spectra for the control (inset) and 6-cyano-2′-deoxy-2′-fluoro-UMP (**35**) treated ODCases. (B) The biochemical transformation of 6-cyano- and 6-cyano-2′-deoxy-2′-fluoro-UMP derivatives by ODCase. In the former case, a hydrolytic process was observed, while in the latter case a covalent complex was observed in the active site of ODCase.

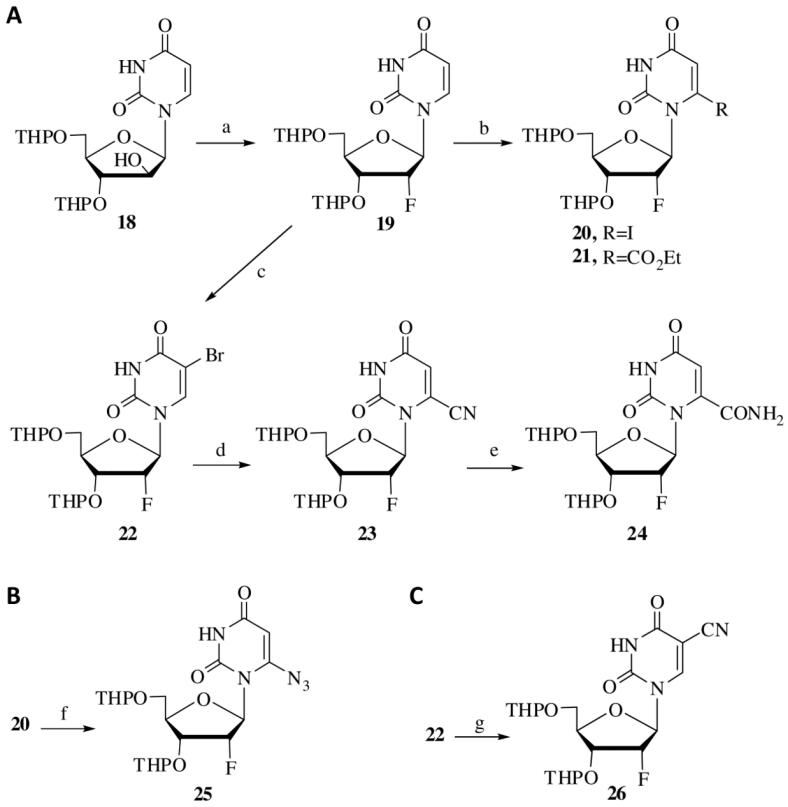

Scheme 1.

Synthesis of 2′-fluoro-6-substituted nucleosides. Reagents: (a) DAST, Pyridine, CH_2Cl_2, 40°C, overnight; (b) LDA, THF, −70°C followed by I_2 or $ClCO_2Et$; (c) NBS, NaN_3, 1,2-dimethoxyethane, rt, overnight; (d) NaCN, DMF, overnight, rt; (e) 1N NaOH, rt, 1 h; (f) NaN_3, DMF; (g) NaCN, DMF, μW @ 150°C, 5 min.

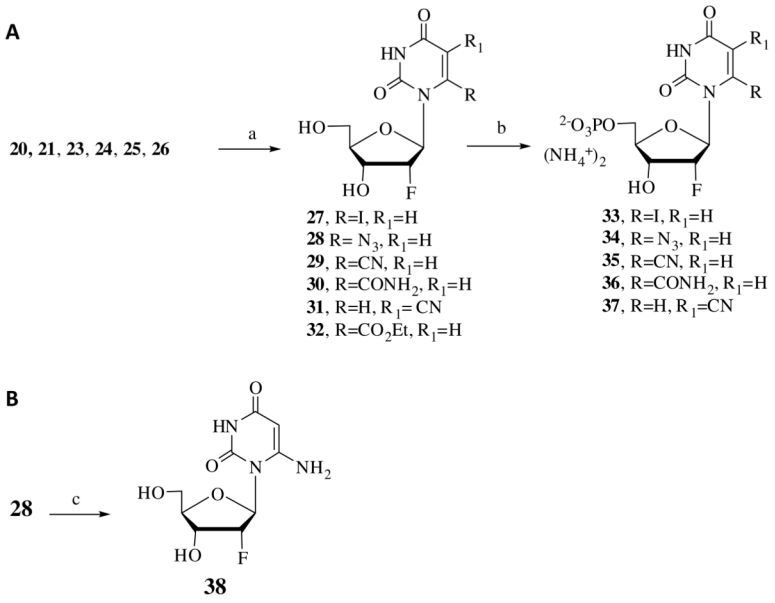

Scheme 2.

Synthesis of 2′-fluoro nucleosides and mononucleotides. Reagents: (a) Amberlite (H^+), H_2O:MeOH (1:1); (b) H_2O/Pyridine/$POCl_3$, CH_3CN, 0°C; (c) H_2, Pd/C.

Table 1

Inhibition kinetics of *Mt* and human ODCases using various 2′-fluorinated uridine nucleotides.

Inhibitor	ODCase K_i (μM)	
	Mt	**human**
6-CN-UMP (**11**)[15,16,17]	28.6 ± 2.1	204 ± 11
6-$CONH_2$-UMP[15,21]	1.32 ± 0.04	-ND-
2′-Deoxy-2′-F-6-CN-UMP (**35**)	37.0 ± 2.5	> 2000
2′-Deoxy-2′-F-6-$CONH_2$-UMP (**36**)	3322 ± 176	> 4000
2′-Deoxy-2′-F-5-CN-UMP (**37**)	360 ± 23	759 ± 88

Table 2

Irreversible inactivation kinetics of *Mt* and human ODCases by 2′-fluoro-6-substituted nucleotides.

Inhibitor	k_{obs}/[I] (M^{-1} sec^{-1})		
	***M. thermoautotrophicum* ODCase**		**Human ODCase**
6-I-UMP (**10**)[16,22]	2.6×10^5		ND
2′-F-6-I-UMP (**33**)	2.0 ± 0.01		0.62 ± 0.02
	K_I (mM)	k_{inact} (hr^{-1})	
5-F-6-N_3-UMP (**12**)[17]	$18.2 \pm 3.6 \times 10^{-3}$	41 ± 3	ND
6-N_3-UMP (**14**)	$6.3 \pm 1.1 \times 10^{-4}$	612	ND
2′-F-6-N_3-UMP (**34**)	1.2 ± 0.1	4.0 ± 0.2	ND
2′-F-6-CN-UMP (**35**)	30 ± 6	2.0 ± 0.2	ND

Table 3

X-ray diffraction data for the co-crystals of 2′-fluoro-6-iodo-UMP (**33**) bound to human ODCase.

Diffraction data		
Resolution (Å)		1.35(1.40–1.35)
Measured reflections (n)		58,884
Unique reflections (n)		56,107
Completeness (%)		94.1(97.7)
R_{sym} (%)		7.3 (47.6)
Space group		$C222_1$
Cell dimensions (Å);	a	78.499
	b	116.0
	c	62.1
Molecules in asymmetric unit (n)		1
Refinement statistics		
Resolution (Å)		50–1.35 (1.35–s1.38)
Protein atoms (n)		2,300
Water molecules (n)		280
Reflections used for R_{free} (n)		2,994 (220)
R_{work} (%)		15.5 (23.8)
R_{free} (%)		17.5 (25.6)
Root mean square deviation bond length (Å)		0.010
Root mean square deviation bond angle (°)		1.44
Average B-factor ($Å^2$)		14.0

Table 4

Antimalarial and anticancer activities of 2′-fluoro-6-substituted nucleosides (expressed as IC_{50} in μM).

Compound	IC_{50} (μM)		
	AML-1	***Pf* (3D7)**	**CHO**
Chloroquine	-	0.022 ± 0.002	-
6-I-uridine[21]	-	6.2 ± 0.7	366 ± 45
5[17]	6.1	-	-
27	> 50	>6000	1363 ± 278
28	>50	>1000	>2000
29	> 50	>1000	>600
30	> 50	>2000	>1000
31	> 50	1090 ± 59	>1000